hdEEG Inverse Source Localisation as A Tool For Studying Nrem Parasomnia

Natalie, NS, Svatkova
Faculty of Biomedical Engineering, Czech Technical University in Prague
natalie.svatkova@gmail.com

Filip, FC, Cerny
Faculty of Biomedical Engineering, Czech Technical University in Prague, National Institute of Mental Health, Klecany
filip.cerny.1@fbmi.cvut.cz

jANA, JK, Koprivova
National Institute of Mental Health, Klecany
jana.koprivova@nudz.cz

JITKA, JB, Buskova
National Institute of Mental Health, Klecany
jitka.buskova@nudz.cz

MAREK, MP, Piorecky
Faculty of Biomedical Engineering, Czech Technical University in Prague, National Institute of Mental Health, Klecany
marek.piorecky@fbmi.cvut.cz

ABSTRACT

The mechanism of brain behaviour outside the parasomnia episode of NREM parasomnia (a sleep disorder) is not fully known. In this study, we examined a group of parasomnia individuals and healthy controls after sleep deprivation. We acquired a dataset containing a simultaneous recording of EEG and fMRI, as well as EEG-only data outside the MR scanner. We used inverse source modelling on the EEG-only data and compared the capability of the method to expose differences between patients and controls with EEG-fMRI data and literature. The results show that the highest difference is in the slow-wave activity of the delta waves, mainly in the occipital region. Even outside the parasomnia episode, differences in fluctuating sleep between patients and controls can be observed.

CCS CONCEPTS

• **Artificial intelligence**; • **Applied computing**; • **Modeling and simulation**;

KEYWORDS

EEG, fMRI, source localisation, NREM parasomnia

ACM Reference Format:
Natalie, NS, Svatkova, Filip, FC, Cerny, jANA, JK, Koprivova, JITKA, JB, Buskova, and MAREK, MP, Piorecky. 2022. hdEEG Inverse Source Localisation as A Tool For Studying Nrem Parasomnia. In *2022 9th International Conference on Bioinformatics Research and Applications (ICBRA 2022), September 18–20, 2022, Berlin, Germany*. ACM, New York, NY, USA, 7 pages. https://doi.org/10.1145/3569192.3569214

ICBRA 2022, September 18–20, 2022, Berlin, Germany

ACM ISBN 978-1-4503-9686-8/22/09.
https://doi.org/10.1145/3569192.3569214

1 INTRODUCTION

Sleep can be characterised by a reduced response to external stimuli, a decreased motion and reduced rate of catabolism [1]. Nowadays, we know that sleep is a nonstationary process, which consists of several parts that repeat multiple times per night in what we call sleep cycles. In an individual sleep cycle, two main phases of electrical brain activity can be observed: NREM (non-rapid eye movement) phase and REM (rapid eye movement) phase. NREM phase can be further divided into three subphases (NREM1-NREM3) according to the dominant frequency of brain electrical activity [2].

Combination of modern recording methods such as simultaneously recorded electroencephalography (EEG) and functional magnetic resonance imaging (fMRI) can provide us with higher resolution on both temporal and spatial level respectively [3]. By this combination of methods, it is possible to localise electrical activity sources of the sleep disorders and based on the origins of the electrical activity deepen the knowledge in this area [4].

1.1 NREM parasomnia

Like other physiological processes, sleep can be disturbed and show abnormalities. Sleep disorders include diagnoses such as insomnia, parasomnia, respiratory disorders (sleep apnoea), movement disorders associated with sleep or excessive sleepiness [5]. However, the neurological background of many of these disorders is still unknown. Parasomnia types of sleep disorders are defined as abnormal behaviours arising from or relating to sleep [6]. These sleep disorders can occur in each sleep phase, with most apparent distinctions between NREM parasomnias and REM parasomnias [7]. NREM parasomnias are also referred to as "Disorders of arousal" (DOAs) [8].

NREM parasomnias have features like complete post-episodic amnesia, the occurrence of the beginning of the episode during the first sleep period, and non-response to external stimuli. The individual episodes of NREM are manifested by abnormal motor behaviour without the presence of brain consciousness. Most commonly NREM parasomnias are observed in sleep with slow wave activity (NREM3) [9].

The pathophysiology of NREM parasomnia has not been fully described yet. NREM parasomnias are thought to be the result of incomplete dissociation between waking and NREM sleep. It should be evaluated if the EEG wave manifested non-physiological states in time of the parasomnia episode.

1.2 EEG and source localization

Electroencephalography (EEG) is a non-invasive method for examining electrical brain activity. Advantage of the method is a high temporal resolution. Problem of this method is spatial resolution as the EEG electrode records activity of multiple neurons from different regions of the brain. Localisation of sources of EEG activity is a type of inverse problem. One solution is the usage of denser electrode layout than the conventional 10-20 system. Today, high density EEGs (hdEEG) with up to 256 electrodes are utilised. Such a number of electrodes can provide us with a set of data robust enough to identify some of the neuronal sources that produced the measured activity. To adequately solve the inverse problem, a properly created realistic forward model of the head is crucial [10, 11]. Based on MRI images we can segment different tissue types and create a proper model of the head with exactly defined head size parameters, electrodes positions and different tissue conductivity inside the model [12]. Areas of the model should span tissue types like grey and white brain matter and cerebrospinal fluid [13]. It has been shown that a complex forward model is more reliable for inverse source reconstruction than a conventional homogeneous tissue model [14, 15].

In this study, a unique data set of patients with NREM parasomnia has been analysed. The aim of the study is to compare the behaviour of the electrical activity of the brain of patients and healthy individuals to reveal different activity at different stages (waking, fluctuating sleep). The main goal is to determine whether the sources of EEG activity differ in individuals with NREM parasomnia.

2 METHODS

This chapter contains the characteristics of the dataset and the measurement conditions. The preprocessing and processing pipeline is also explained as well as the method of EEG source localisation based on eLORETA.

2.1 Dataset

A total of 20 individuals participated in the study (10 patients diagnosed with NREM parasomnia and 10 healthy controls).

The experiment took place at the National Institute of Mental Health (NIMH) and was approved by the local Ethics Committee of the NIMH (approval code: 185/17). Patients were diagnosed based on an overnight video-polysomnography (vPSG). The NREM parasomnia diagnosis was based on ICSD-3 criteria (American Association Of Sleep Medicine, 2014). The study processes data from simultaneous EEG-fMRI measurements and subsequent EEG-only out-of-scanner measurements. Subjects were sleep deprived for 28h ± 1 h. Due to technical complications in measurement, 2 patients were excluded from simultaneous measurement. For a subsequent EEG-only measurement, 5 NREM parasomnia patients and 4 control subjects were selected.

All procedures followed the ethical standards of the responsible Committee for Experimentation with Humans (institutional and national) and with the Declaration of the World Medical Association of Helsinki on the Ethical Principles of Medical Research Involving Human Subjects.

The MR compatible Geodesic EEG System (GES) 400 from Electrical Geodesics, Inc. (EGI) was used to measure EEG. The system includes a Net Amps 400 amplifier, controlled by an iMac with Net Station software, and synchronisation is controlled by GES Clock Sync I/O. It also includes shielding (Field Isolation Containment System, FICS) and input filtering, which significantly reduces the effect of MR noise sources. EGI 256-channel EEG system uses only 1 reference electrode marked Ref Cz. The sampling frequency of raw data was 1000 Hz. An MR device with a static magnetic field size of 3T from Siemens, model Siemens Magneton Prisma, was used for the measurement. Anatomical images from the MP-RAGE (T1) sequence were used for EEG electrode co-registration.

2.2 Preprocessing

Data processing was performed in MATLAB. FieldTrip toolbox [16] was used together with the AAL atlas, as well as EEGLAB and SimBi toolboxes. As part of the data preprocessing, the recorded EEG datasets were downsampled from 1 kHz to 250 Hz. This step was performed in order to reduce the size of each recording. The sampling frequency was reduced using cubic Hermitian polynomials. Subsequently, high-amplitude artifacts were removed from the records, which could adversely affect the following analysis. The recordings were then filtered using a bandpass FIR filter with cut-off frequencies of 0.3 Hz lower and 30.0 Hz upper. The filter order was 1650. A two-way filter was selected to prevent phase shift. An isoline shift filter was also used. The Independent Component Analysis (ICA) method was used to remove some other artifacts, especially the eye-induced artifact. Components were selected based on time series and topographic maps. Locations in the frontal area of the topographic map are typical for eye artifacts, and in the time series, they also manifest as high-amplitude waves. Selected artifact related components have been removed. The recordings were segmented into 30-second-long sections with zero overlaps.

2.3 Spectral analysis

Frequency analysis was performed for every 30 second segment using the Fast Fourier Transform (FFT). The output of the frequency analysis consisted of power and cross power spectra. The frequency resolution was set to 0.5 Hz. The frequency range of interest was selected from 0.5 Hz to 30 Hz. A total of 4 EEG bands were distinguished in this frequency region of interest: delta (0.5 - 4.0 Hz), theta (4.0 - 7.5 Hz), alpha (8.0 - 13.0 Hz), and beta (14.0 - 30.0 Hz). Thus, for each frequency from 0.5 Hz to 30 Hz in 0.5 Hz steps, the average power value at that frequency across each segment was calculated. Hanning's windows were used to calculate the frequency analysis. To suppress intersubject variability, the spectrum was normalised, and the resulting relative values ranged from 0-1.

2.4 Criterion based selection

For each subject, the individual 30-second segments were divided into 3 groups based on the ratio of delta band power to theta band

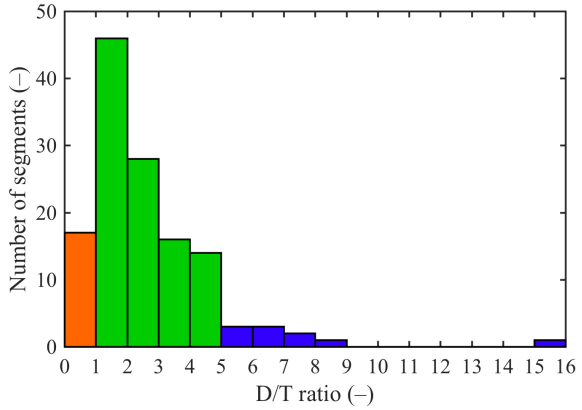

Figure 1: Illustration of division of intrasubject trials into groups, based on D/T spectral powers ratio.

power (D/T ratio). Segments with a D/T ratio of less than one are in the first (orange) group, see figure 1. Here, the power in the theta band is greater than the power in the delta band. The boundary between the second (green) group and the third (blue) group was further determined using a histogram. This limit was determined as the "knee" of the histogram, i.e. the site of the most significant change in frequency. Source localisation and subsequent statistical evaluation were performed only for the first and second group. The third group contained largely outliers.

2.5 Source localization

The forward model estimates the potential on the surface of the head for a known source and a known model of the head. The result of the forward problem is the so-called lead model matrix, which describes the field propagation on the electrodes for a given source. The computational brain model (headmodel, see Figure 2) was created on the basis of anatomical MRI images and known conductivities of individual tissues. The anatomical MRI images used were T1-weighted images, which were first segmented. When segmenting anatomical MRI images, a total of 5 tissue types were distinguished: skin, skull, cerebrospinal fluid, white matter, and grey matter. MRI image segmentation was performed using the SPM toolbox. A 3D geometric description of the head was created directly from the segmented MRI images using a hexahedral mesh. The points of the hexahedral network form hexagons, where each hexahedron is assigned to exactly one tissue type. An offset parameter of 0.3 was used. Thanks to the offset parameter, a smoother display of the boundaries and a better approximation of the actual head shape are achieved.

The conductivities of the individual tissues for creating the computational model of the brain are specified in Table 1. From the geometric description of the head and electrical information about individual tissues, the computational model of the brain itself was subsequently created using the finite element method (FEM) using the SimBio toolbox integrated into the FieldTrip toolbox. The dipoles are approximated in model by the approach of St. Venant.

Table 1: Conductivities of head tissues used in creation of the brain model.

Type of tissue	Conductivity
Scalp tissue	0.43
Skull	0.01
Cerebrospinal fluid	1.79
White brain matter	0.14
Grey brain matter	0.33

The source model was created using a regular 3D grid with a resolution of 7 mm in all directions. The resource model was co-registered with the computational brain model (headmodel). The head model, electrode, and source model were registered in the same coordination system using three anatomical reference points.

The eLORETA method is a discrete method that calculates the weighted inverse solution in 3D space, i.e., the localisation of resources based on the potential distribution on the scalp [17] . The specific scales used in eLORETA give tomography the property of precise localisation and current density image [18]. Neighbouring neural sources are highly correlated, so spatial resolution is low.

2.6 Comparison with EEG-fMRI data

Resulting sources of EEG activity were compared to results from the data recorded with simultaneous EEG-fMRI. The processing pipeline used for this dataset was previously published and is further specified in article [19]. Datasets were measured just before the EEG-only measurement and consist of 7 NREM parasomnia patients and 8 control subjects.

2.7 Statistical analysis

The values of the percentage of total power in the individual EEG bands were statistically evaluated using a permutation test. The number of permutations was chosen to be 100,000. At the significance level of 0.05, the null hypothesis was set to no statistically significant difference between EEG patients and control group during sleep at the selected level of significance in the representation of power in the given band. The output of the statistical permutation test consisted of 3 values: p-value, observed difference, and Hedges' g. Hedges' g indicates the degree of effect on how different a group of patients differs from a group of controls. The value of Hedges' g is calculated according to the equation:

$$g = \frac{x_1 - x_2}{s^*} \tag{1}$$

Where x1 is the mean of group 1, x2 is the mean of group 2 and s* is pooled standard deviation.

Statistical differences between patients and control group were estimated using a non-parametric both-side MonteCarlo test with cluster-based correction. The significance level was set at 5 %.

3 RESULTS

The study examined data from patients with NREM parasomnias. EEG records of fluctuating sleep were compared between patients and healthy controls. NREM parasomnia is manifested mainly in

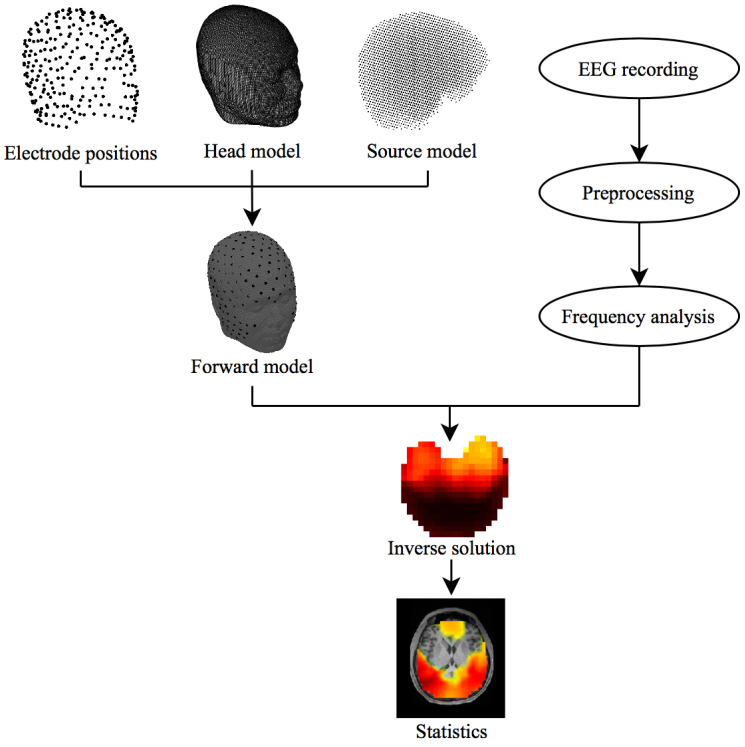

Figure 2: The localization of sources takes place in parallel in two branches. A model is created for estimating the current paths to the source and at the same time EEG data are preprocessed and then modelled into the source using a prepared model.

Table 2: Statistical evaluation of percentage of total power in studied EEG frequency bands.

EEG frequency band	p-value	Observed difference	Hedge's g
Alpha	0.7500	0.2559	0.0194
Beta	0.00140	-0.9429	-0.1940
Delta	0.00650	-3.0006	-0.1662
Theta	0.00006	3.0060	0.2464

the NREM3 stage of sleep [9]. In the study, we asked the hypothesis whether differences in fluctuating sleep (wake transition - light and deeper sleep) could be found outside the parasomnia episode. The most significant difference was observed in the delta band, see table 2. Based on our previous study, we also included the theta band in source localization.

3.1 Distribution of D/T ratios

Recorded hdEEG data were preprocessed utilising the pipeline mentioned in the methods section. 5 NREM parasomnia patients and 4 control subjects were selected for a further source localisation process. For each patient a D/T ratio was computed to divide the ongoing brain activity into a deep sleep category and light sleep or wakefulness category. Table 3 shows the distribution of D/T ratio among the subjects. We chose the delta-theta ratio because it is used to determine the depth of sleep [20]. It is not clear whether physiology is maintained in this regard in NREM parasomnias, however, sleep is scored as standard [21]. Therefore, we divided the data into only 2 mentioned categories. Table 3 shows that two patients and one control spent significantly more time in sleep. Outliers are homogeneous in patients and controls.

3.2 eLORETA results

Using source localisation, we searched for different activations between a group of patients and controls (figure 3). Greater activity in the theta control group is propagated closer to the cortex surface in the anteroposterior direction [22]. In this way, slow waves typical of physiological sleep are propagated regularly [23]. However, the group of patients has a significantly higher activity in this zone in the temporal area. There is more activity in the delta band in a group of patients who could be in a state of deeper sleep.

Table 3: D/T ratios across subjects in NREM parasomnia patients group and control group.

Group of subjects		Orange D/T ratio(theta> delta)	Green D/T ratio(delta> theta)	Blue D/T ratio(outliers)
Patients	1	80	25	15
	2	32	57	3
	3	12	96	8
	4	17	104	10
	5	51	72	9
Controls	1	71	47	17
	2	12	107	15
	3	69	49	16
	4	2	74	9

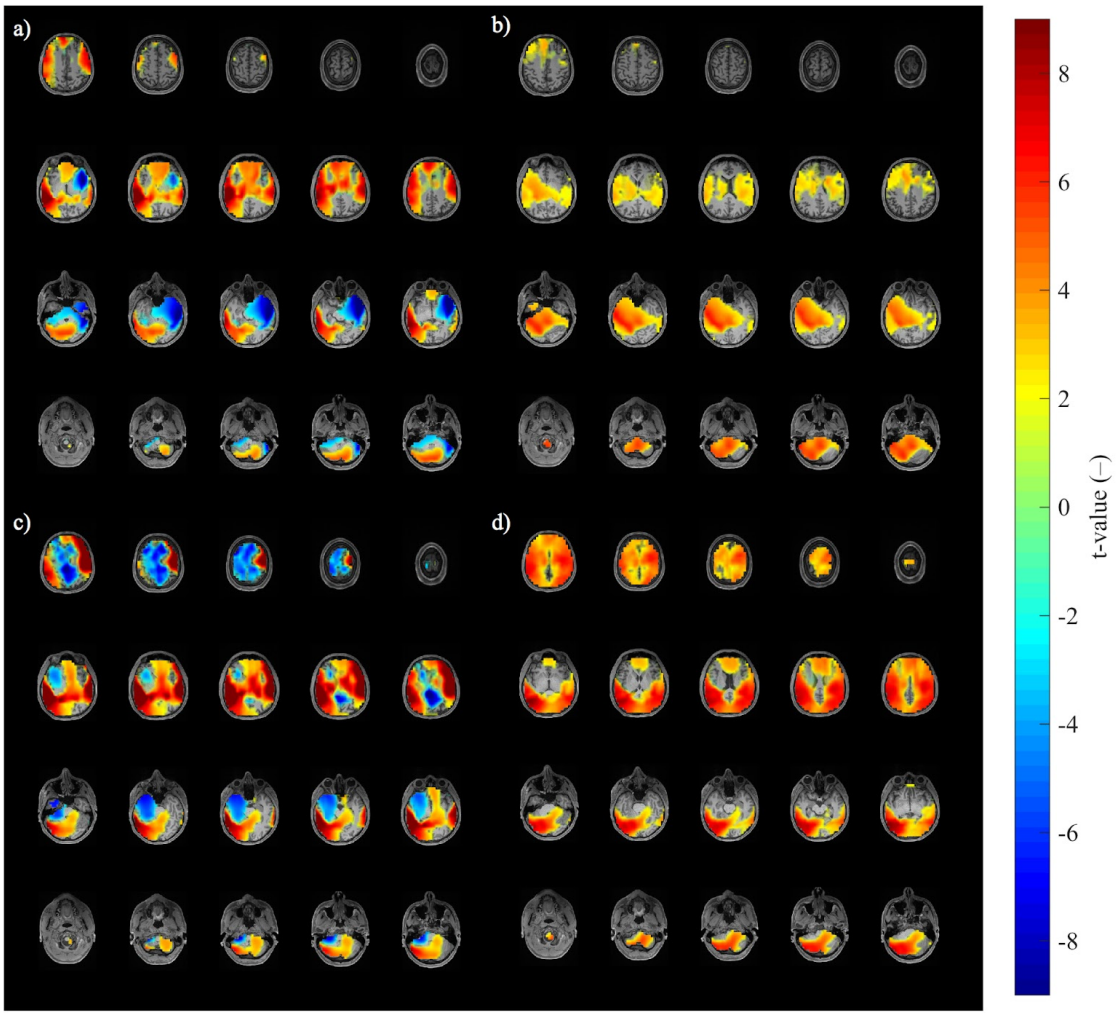

Figure 3: Group analysis of significant brain region activity. a) Green D/T area for theta spectral power b) for delta spectral power. c) Orange D/T area for theta spectral power d) for delta spectral power. Visualised is the difference in the direction patients

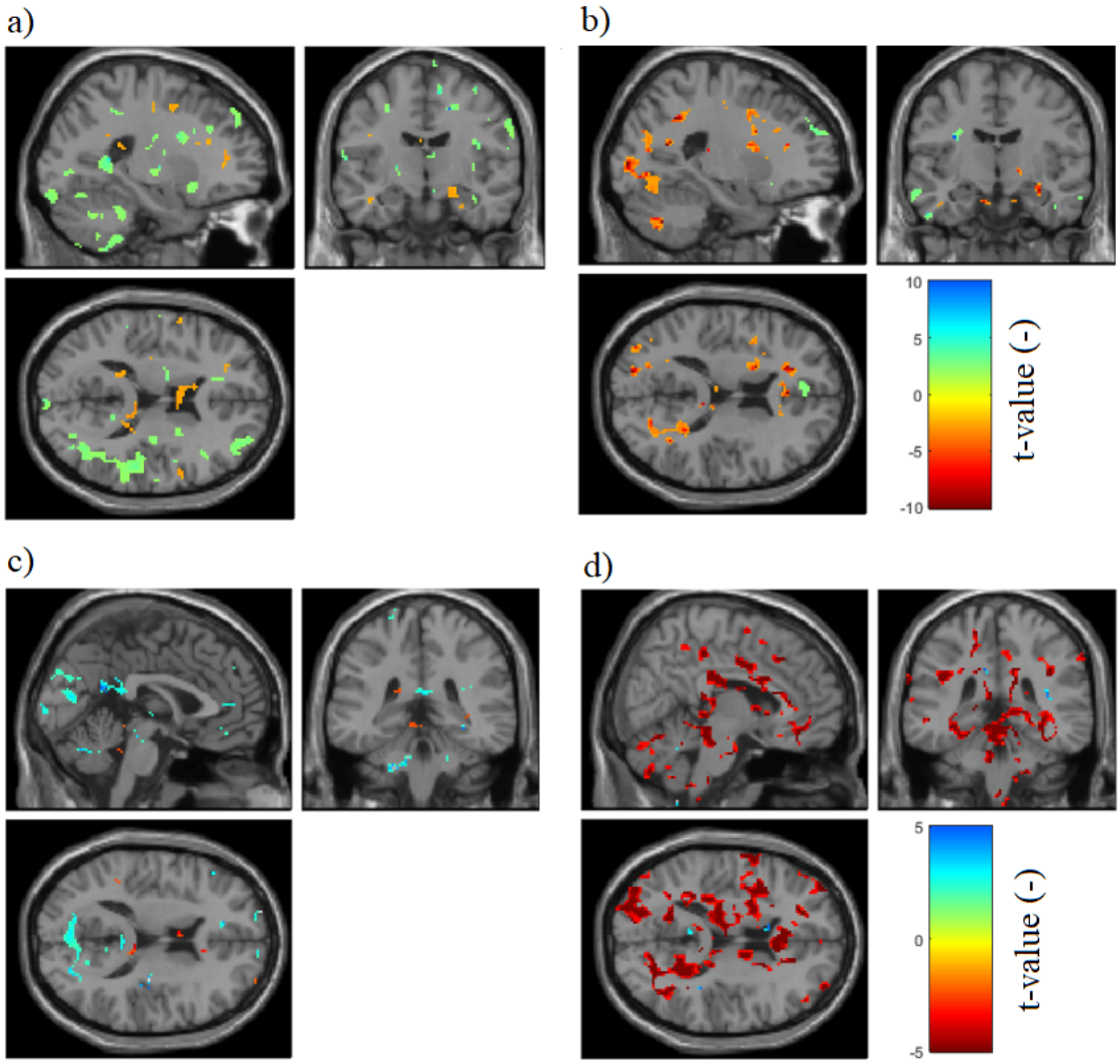

Figure 4: Results of simultaneous EEG-fMRI recordings. Visualised is the difference between power spectrum fluctuations and spontaneous fluctuations of fMRI BOLD signal: a) Theta power spectrum of control subjects (n=8), b) Theta power spectrum of patients (n=7)

3.3 Comparison with simultaneous EEG-fMRI recordings

Brain activations described in the previous section were compared to results of simultaneously acquired EEG-fMRI dataset of NREM parasomnia patients and control subjects (figure 4). Source localisation based on EEG-fMRI data is more precise than EEG-only measurement, therefore we can use it as a reference to whether our EEG-only results are in compliance with a more robust method. One limitation is a different sample size (n=15), which was greater than EEG-only measurement (n=9). However, we chose to compare the results, because the EEG-fMRI measurement preceded the EEG-only measurement and the data were recorded with the same EEG cap, which was not removed or adjusted between the experiments. [19]

Source localisation is very sensitive to interference, which can lead to false-positive localisations. Therefore, source localisation of the EEG recorded within the magnetic resonance is a demanding process in terms of artifact residues. Because of this, we asked the subjects to try to sleep also outside the MR scanner (after about one hour of simultaneous EEG and fMRI examinations). Limitation of the study is the small sample size used for inverse source localisation. This is based on the fact that NREM parasomnias are rare diseases with a prevalence in adults of around 7 % [3]. Also, not all subjects underwent the second part - sleeping outside of the MR scanner.

We used several types of corrections of multiple comparisons for EEG source localisation. Bonferroni correction returned no significant areas. FDR and cluster corrections, which are less strict, gave similar results. In the future, the source dataset needs to be expanded to disprove the impact of the low number of subjects, where one remote subject may skew the results.

The EEG does not have spatial resolution as good as the fMRI, so the locations found have probably larger volume than the actual signal source. However, common regions were found in comparison with EEG-fMRI data, specifically in motor cortex and occipital regions. Thus, it is possible that these regions like angular gyrus and its surroundings may excite or inhibit the activity of NREM parasomnias. Angular gyrus is assumed to be an integration centre of auditory, visual, and somatosensory information [24]. These functions could also play a role in NREM parasomnias attack because people could hear and have some visual sense.

4 CONCLUSION

We utilised EEG source localisation on a group of NREM parasomnia patients. In the activity of NREM parasomnia patients group we observed unusual activity in the delta band in the temporal brain region. This deviation was not observed in the group of control subjects. As a reference to our results, we compared the data with previously published simultaneous EEG-fMRI NREM parasomnia study on the same dataset. In the future, it should be considered to perform the analysis on a wider set of subjects.

ACKNOWLEDGMENTS

This work was supported by the Grant Agency of the Czech Technical University in Prague, reg. no. SGS22/200/OHK4/3T/17 and SGS21/140/OHK4/2T/17.

REFERENCES

[1] Saeid Sanei and J.A. Chambers. EEG Signal Processing. DOI:https://doi.org/10.1002/9780470511923

[2] 2005. *The international classification of sleep disorders : diagnostic & coding manual.* (2nd ed ed.). American Academy of Sleep Medicine, Westchester, IL..

[3] Elias Ebrahimzadeh, Mohammad Shams, Masoud Seraji, Seyyed Sadjadi, Lila Rajabion and Hamid Soltanian-Zadeh. 2021. Localizing Epileptic Foci Using Simultaneous EEG-fMRI Recording: Template Component Cross-Correlation. *Frontiers in Neurology* vol. 12, (2021).. DOI:https://doi.org/10.3389/fneur.2021.695997

[4] CXi-Jian Dai, Jihui Zhang, Yongjun Wang, Yan Ma and Kuangyu Shi. 2021. Editorial: EEG and fMRI for Sleep and Sleep Disorders–Mechanisms and Clinical Implications. Frontiers in Neurology vol. 12, (2021). DOI:https://doi.org/10.3389/fneur.2021.749620

[5] Michael J Sateia. 2014. International Classification of Sleep Disorders-Third Edition. Chest vol. 146, issue 5 (2014), 1387-1394. DOI:https://doi.org/10.1378/chest.14-0970

[6] Michael J. Howell. 2012. Parasomnias: An Updated Review. Neurotherapeutics vol. 9, issue 4 (2012), 753-775. DOI:https://doi.org/10.1007/s13311-012-0143-8

[7] Shantanu Singh, Harleen Kaur, Shivank Singh and Imran Khawaja. Parasomnias: A Comprehensive Review. Cureus.. DOI:https://doi.org/10.7759/cureus.3807

[8] Anna Castelnovo, Régis Lopez, Paola Proserpio, Lino Nobili and Yves Dauvilliers. 2018. NREM sleep parasomnias as disorders of sleep-state dissociation. Nature Reviews Neurology vol. 14, issue 8 (2018), 470-481. DOI:https://doi.org/10.1038/s41582-018-0030-y

[9] Panagis Drakatos, Lucy Marples, Rexford Muza, Sean Higgins, Nadia Gildeh, Raluca Macavei, Eptehal Dongol, Alexander Nesbitt, Ivana Rosenzweig, Elaine Lyons, Grainne d'Ancona, Joerg Steier, Adrian Williams, Brian Kent and Guy Leschziner. 2019. NREM parasomnias: a treatment approach based upon a retrospective case series of 512 patients. Sleep Medicine vol. 53, (2019), 181-188. DOI:https://doi.org/10.1016/j.sleep.2018.03.021

[10] Zoltan J. Koles. 1998. Trends in EEG source localization. Electroencephalography and Clinical Neurophysiology vol. 106, issue 2 (1998), 127-137. DOI:https://doi.org/10.1016/S0013-4694(97)00115-6

[11] Shiva Asadzadeh, Tohid Yousefi Rezaii, Beheshti, Azra Delpak and Meshgini. 2020. A systematic review of EEG source localization techniques and their applications on diagnosis of brain abnormalities. Journal of Neuroscience Methods vol. 339, (2020). DOI:https://doi.org/10.1016/j.jneumeth.2020.108740

[12] Christoph Michel and Bin He. 2019. EEG source localization. Clinical Neurophysiology: Basis and Technical Aspects (2019), 85-101. DOI:https://doi.org/10.1016/B978-0-444-64032-1.00006-0

[13] Johannes Vorwerk, Jae-Hyun Cho, Stefan Rampp, Hajo Hamer, Thomas Knösche and Carsten Wolters. 2014. A guideline for head volume conductor modeling in EEG and MEG. NeuroImage vol. 100, (2014), 590-607. DOI:https://doi.org/10.1016/j.neuroimage.2014.06.040

[14] Jae-Hyun Cho, Johannes Vorwerk, Carsten Wolters and Thomas Knösche. 2015. Influence of the head model on EEG and MEG source connectivity analyses. NeuroImage vol. 110, (2015), 60-77. DOI:https://doi.org/10.1016/j.neuroimage.2015.01.043

[15] Frank Neugebauer, Gabriel Möddel, Stefan Rampp, Martin Burger and Carsten Wolters. 2017. The Effect of Head Model Simplification on Beamformer Source Localization. Frontiers in Neuroscience vol. 11, (2017). DOI:https://doi.org/10.3389/fnins.2017.00625

[16] 2020. Fieldtrip. Retrieved 2021-01-08 from https://www.fieldtriptoolbox.org/

[17] R. D. Pascual-Marqui. 2007. Discrete, 3D distributed, linear imaging methods of electric neuronal activity. Part 1: exact, zero error localization. (2007). DOI:https://doi.org/10.48550/arXiv.0710.3341

[18] Roberto D. Pascual-Marqui. 2009. Theory of the EEG Inverse Problem, Chapter 5, pp: 121-140. Quantitative EEG Analysis: Methods and Clinical Applications (2009).

[19] Marek Piorecky, Vlastimil Koudelka, Eva Miletinova, Jitka Buskova, Jan Strobl, Jiri Horacek, Martin Brunovsky, Stanislav Jiricek, Jaroslav Hlinka, David Tomecek and Vaclava Piorecka. 2020. Simultaneous fMRI-EEG-Based Characterisation of NREM Parasomnia Disease: Methods and Limitations. Diagnostics vol. 10, issue 12 (2020).. DOI:https://doi.org/10.3390/diagnostics10121087

[20] Sophie Bagur, Marie Lacroix, Gaëtan de Lavilléon, Julie Lefort, Hélène Geoffroy, Karim Benchenane and Igor Timofeev. 2018. Harnessing olfactory bulb oscillations to perform fully brain-based sleep-scoring and real-time monitoring of anaesthesia depth. PLOS Biology vol. 16, issue 11 (2018). DOI:https://doi.org/10.1371/journal.pbio.2005458

[21] Milena Camaioni, Serena Scarpelli, Maurizio Gorgoni, Valentina Alfonsi and Luigi De Gennaro. 2021. EEG Patterns Prior to Motor Activations of Parasomnias: A Systematic Review. Nature and Science of Sleep Volume 13, (2021), 713-728. DOI:https://doi.org/10.2147/NSS.S306614

[22] M. Massimini. 2004. The Sleep Slow Oscillation as a Traveling Wave. Journal of Neuroscience vol. 24, issue 31 (2004), 6862-6870. DOI:https://doi.org/10.1523/JNEUROSCI.1318-04.2004

[23] Igor Timofeev, Sarah Schoch, Monique LeBourgeois, Reto Huber, Brady Riedner and Salome Kurth. 2020. Spatio-temporal properties of sleep slow waves and implications for development. Current Opinion in Physiology vol. 15, (2020), 172-182. DOI:https://doi.org/10.1016/j.cophys.2020.01.007

[24] Marc D. Binder and Nobutaka Hirokawa. 2009. Causality, Mental. Encyclopedia of Neuroscience (2009), 587-587. DOI:https://doi.org/10.1007/978-3-540-29678-2_856